Kinetics of the Ca^{2+}, H^+, and Mg^{2+} Interaction with the Ion-Binding Sites of the SR Ca-ATPase

Christine Peinelt and Hans-Jürgen Apell
Department of Biology, University of Konstanz, 78457 Konstanz, Germany

ABSTRACT Electrochromic styryl dyes were used to investigate mutually antagonistic effects of Ca^{2+} and H^+ on binding of the other ion in the E_1 and P-E_2 states of the SR Ca-ATPase. On the cytoplasmic side of the protein in the absence of Mg^{2+} a strictly competitive binding sequence, $H_2E_1 \rightleftharpoons HE_1 \rightleftharpoons E_1 \rightleftharpoons CaE_1 \rightleftharpoons Ca_2E_1$, was found with two Ca^{2+} ions bound cooperatively. The apparent equilibrium dissociation constants were in the order of $K_{1/2}$(2 Ca) = 34 nM, $K_{1/2}$(H) = 1 nM and $K_{1/2}(H_2)$ = 1.32 μM. Up to 2 Mg^{2+} ions were also able to enter the binding sites electrogenically and to compete with the transported substrate ions ($K_{1/2}$(Mg) = 165 μM, $K_{1/2}(Mg_2)$ = 7.4 mM). In the P-E_2 state, with binding sites facing the lumen of the sarcoplasmatic reticulum, the measured concentration dependence of Ca^{2+} and H^+ binding could be described satisfactorily only with a branched reaction scheme in which a mixed state, P-E_2CaH, exists. From numerical simulations, equilibrium dissociation constants could be determined for Ca^{2+} (0.4 mM and 25 mM) and H^+ (2 μM and 10 μM). These simulations reproduced all observed antagonistic concentration dependences. The comparison of the dielectric ion binding in the E_1 and P-E_2 conformations indicates that the transition between both conformations is accompanied by a shift of their (dielectric) position.

INTRODUCTION

Contraction and relaxation of muscle fibers is controlled by the cytoplasmic Ca^{2+} concentration, which is changed mainly by the release of Ca^{2+} through ion channels from, and its uptake into, the sarcoplasmatic reticulum (SR), the main storage compartment of Ca^{2+} ions, by the SR Ca-ATPase. To provide muscle relaxation, the cytoplasmic Ca^{2+} concentration has to be reduced from ~10 μM to below 0.1 μM in time intervals as short as 50 ms. This powerful uphill transport of Ca^{2+} is mainly performed by SR Ca^{2+} pumps, which constitute more than 70% of the proteins in the SR membrane and which reach a density in this membrane of about 30,000 μm^{-2} (Franzini-Armstrong and Ferguson, 1985). In accordance with its importance for living organisms, studies on structural and mechanistic properties of the SR Ca-ATPase are numerous, and this protein is one of the best-investigated ion pumps (Inesi et al., 1995; Menguy et al., 1998; MacLennan et al., 1997; Martonosi, 1995; Møller et al., 1996; Vilsen, 1995). Recently, the crystal structure of the SR Ca-ATPase in its E_1 conformation was published with a resolution of 2.6 Å as the first of the P-type ATPases (Toyoshima et al., 2000), which allows a detailed insight into possible structure–function relations.

To understand the ion transport mechanism of the pump, a number of features from the published structure are important. It was found that, in the E_1 conformation of the Ca-ATPase, both ions are located side by side with a distance of 5.7 Å, approximately in the middle of the transmembrane section of the protein (Toyoshima et al., 2000). This structural arrangement is in agreement with the observation of electrogenic binding of Ca^{2+} and H^+ to the pump in its E_1 conformation (Butscher et al., 1999). From the crystal structure of the Ca-ATPase in the P-E_2 conformation with lower resolution (8 Å) also, a position of the Ca^{2+} ions deep inside the membrane section was proposed (Zhang et al., 1998). This observation suggests that, in the P-E_2 conformation, the transmembrane segments that form the ion binding sites may not be dramatically shifted relative to their position in the E_1 conformation. In functional studies, it was found that Ca^{2+} binding from the luminal side of the membrane is also electrogenic (Butscher et al., 1999). The high-resolution structure revealed that the ion binding sites are surrounded by the transmembrane helices M4–M6 and M8, that the α helices M4 and M6 are partly unwound and provide thus an efficient coordination geometry for the two Ca^{2+} ions. A cavity with a rather wide opening, surrounded by M2, M4, and M6 is discussed as an access structure on the cytoplasmic side. The outlet of Ca^{2+} on the luminal side is likely to be located in the area surrounded by M3–M5.

From kinetic studies, it is known that the Ca-ATPase works under physiological conditions as an ion exchanger with a stoichiometry of 2 Ca^{2+}/2 H^+ per ATP hydrolyzed (Yu et al., 1993, 1994; Yu and Inesi, 1995). Binding of the two Ca^{2+} ions in E_1 is strictly sequential, and the properties of both sites are not equivalent (Inesi and de Meis, 1989; Inesi et al., 1990). It was also found that the second divalent cation, Mg^{2+}, which is present under physiological conditions with considerable concentrations in the cytoplasm, also interacts with the ion binding sites and affects Ca^{2+} binding (Forge et al., 1993), although it is not transported (Forge et al., 1995).

Direct studies of the ion transport with electrophysiological techniques are not possible because of the high leak

Received for publication 26 June 2001 and in final form 16 August 2001.
Address reprint requests to Hans-Jürgen Apell, University of Konstanz, Dept. of Biology, Fach M635, 78457 Konstanz, Germany. Tel.: +49-7531-88-2253; Fax: +49-7531-88-3183; E-mail: h-j.apell@uni-konstanz.de.

0006-3495/02/01/170/12 $2.00

conductance of the SR membranes for all monovalent ions. The reconstitution of the SR Ca-ATPase in lipid vesicles and the use of fluorescent dyes as indicators for membrane potential, Ca^{2+} concentration and pH proved elegantly and convincingly the electrogenicity of the ion pump and the stoichiometry mentioned above (Yu et al., 1993, 1994). However, insights into partial reactions of the pump cycle are rather restricted in the case of investigations with proteoliposomes based on the use of fluorescent indicators that detect ion concentrations or membrane potential (Apell and Bersch, 1987).

To study electrogenic partial reactions in ion pumps, such as Na,K-ATPase and SR Ca-ATPase, fluorescent styryl dyes have been introduced as a suitable approach (Apell et al., 1996; M. Pedersen, M. Roudna, S. Beutner, M. Birmes, B. Reiters, H.-D. Martin, and H.-J. Apell, submitted for publication; Butscher et al., 1999; Klodos and Forbush, 1988; Schneeberger and Apell, 1999; Stürmer et al., 1991; Clarke et al., 1998). The detection mechanism of styryl dyes is based mainly on their electrochromic behavior under specific experimental conditions, i.e., low dye concentrations in the order of 200 nM, and excitation at the red edge of the absorption spectrum (M. Pedersen, M. Roudna, S. Beutner, M. Birmes, B. Reiters, H.-D. Martin, and H.-J. Apell, submitted for publication; Bühler et al., 1991). This means that an observed fluorescence decrease or increase occurs when positive charge is imported into or is removed from the protein, respectively. Since the styryl dyes report essentially the change of local electric fields within the protein/membrane dielectric, and to a lesser extent transmembrane electric potentials, this method can be well applied to open membrane fragments (as in the case of the Na,K-ATPase) or to leaky vesicular membranes (as in the case of SR membranes).

In this presentation, we want to show and discuss detailed results of the interaction of the physiologically relevant cations at the ion binding sites of the Ca-ATPase in both its principal conformations with respect to the known structural details and their implications on the mechanism of ion transport.

MATERIALS AND METHODS

Phosphoenolpyruvate, pyruvate kinase, lactate dehydrogenase, A23187, NADH, ATP (disodium salt, special quality) were from Boehringer (Mannheim, Germany). Tharpsigargin was purchased from Sigma (München, Germany). BAPTA (1,2*bis*(2-aminophenoxy)-ethane-*N*,*N*,*N*′,*N*′ tetrasodium salt) was obtained from MoBiTec (Göttingen, Sweden), EGTA (Ethylenglycol O,O′-*bis*(2-aminoethyl)-*N*,*N*,*N*′,*N*′ tetraacetic acid) from Fluka (Buchs, Switzerland). KCl (suprapure quality) and all other reagents (at least analytical grade) were from Merck (Darmstadt, Germany). 2BITC (1-[4-isothiocyanato-*n*-butyl]-4-[(p-*N*,*N*-diethylamino)styryl]pyridinium bromide) and 2HITC (1-[4-isothiocyanato-*n*-hexyl]-4-[(p-*N*,*N*-diethylamino)styryl]pyridinium bromide) were synthesized in the Institute of Organic Chemistry and Macromolecular Chemistry at the University of Düsseldorf, Germany, by M. Birmes and S. Beutner, according to Birmes (1995).

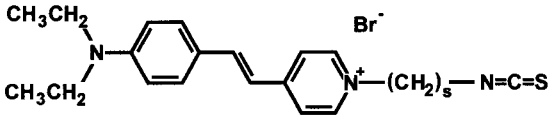

FIGURE 1 Chemical structure of the styryl dyes applied in the presented experiments to detect charge movements in the SR Ca-ATPase. 2BITC has a spacer length of $s = 4$, and 2HITC has a spacer length of $s = 6$.

SR Ca-ATPase was prepared by a slight modification of the method of Heilmann et al. (1977) from the psoas muscle of rabbits. The whole procedure was performed at temperatures below 4°C. The determination of the protein content of the membrane preparation was performed according to Markwell et al. (1978). The most active fractions of the final density gradient separation had a protein content of 2–3 mg/ml. The enzymatic activity was determined by the linked pyruvate kinase/lactate dehydrogenase assay (Schwartz et al., 1971) in a buffer containing 200 μM of free Ca^{2+}. Background enzymatic activity of the isolated preparation was obtained by addition of 1 μM tharpsigargin. The Ca-ATPase specific activity was ~1.8 units/mg at 20°C and pH 7.5 (which corresponds to 1.8 μmol ATP hydrolyzed per mg protein per min) and could be increased to 2.6 units/mg in the presence of A23187 to short-circuit the membranes for Ca^{2+}. With a molar weight 110,000 g/mol and a specific activity of 1.8 units/mg, the turnover rate of the pump is 0.33 s^{-1} in this preparation.

Fluorescence measurements were performed with two setups. In the first setup, a commercial fluorescence spectrometer LS 50B (Perkin Elmer, Überlingen, Germany), ion-transport-specific data were obtained by experiments in quartz cuvettes of 1 or 2 ml effective volume. The cuvette holder was thermostated at 20°C and equipped with a magnetic stirrer. The experiments with the styryl dye 2BITC were performed as described previously (Butscher et al., 1999). With the alternative dye, 2HITC, the same settings could be used (Fig. 1). The dye concentration was 200 nM throughout, the excitation wavelength was 545 nm (slit width 15 nm), and the emission wavelength 590 nm (slit with 20 nm) for both dyes. The second setup was self-constructed. It used a HeNe laser with a wavelength of 543 nm to excite the fluorescence of both dyes. The emitted light was collected perpendicular to the incident light, filtered by a narrow-band interference filter (λ_{max} = 589 nm, half width 10.6 nm; Dr. Hugo Anders, Nabburg, Germany) and detected by a head-on photo multiplier (R1387, Hamamatsu, Japan). The amplified photo current was collected by a data-acquisition board of a PC with sampling frequencies between 1 and 10 Hz, displayed and analyzed on the computer. The temperature in the cuvette (2 ml) was maintained accurately by a Peltier thermostat at 20°C.

Although, at physiological pH, the substrate-induced fluorescence changes are comparable for both styryl dyes, the responses on H^+ binding are slightly more pronounced in the case of 2HITC. Free Ca^{2+} concentrations were calculated with the program Winmaxc V.2.0 (http//www.stanford.edu/~cpatton). To solve systems of linear equations modeled for the analysis of experimental data and to find fitting solutions, the program system Mathematica V.4.1 and Mathcad 2000 Pro were used.

RESULTS

On the basis of the observation that ion binding to and release from the Ca-ATPase are electrogenic events in both principal conformations, E_1 and P-E_2, electrochromic fluorescence dyes may be used to study the kinetics of the interaction of ions and ion pump as well as the competition between ions for the sites (Butscher et al., 1999). To study the effect of various partial reactions on the applied dyes, a

series of experiments was performed to compare their responses to different ionic conditions.

Ion binding to the cytoplasmic ion sites

The first set of experiments was performed to investigate binding and competition of Ca^{2+}, Mg^{2+}, and H^+ in the E_1 conformation of the SR Ca-ATPase. This conformation is maintained if ions are added in the absence of ATP and inorganic phosphate, P_i.

The standard experiment (Fig. 2 *A*) was performed in buffer of 25 mM tricine, 50 mM KCl, 1 mM $MgCl_2$, pH 7.2. After the incubation of 200 nM 2HITC and membranes containing 19.4 μg/ml Ca-ATPase in the buffer (until a stationary level of fluorescence was reached) the Ca^{2+}-specific chelator BAPTA was added to a final concentration of 100 μM. Because the initial buffer contained ~4.5 μM free Ca^{2+}, the fluorescence increase upon addition of BAPTA reflects the reaction $Ca_xE_1 \rightarrow E_1$, where x has an (averaged) value between 1 and 2 (Butscher et al., 1999). Subsequent addition of 300 μM $CaCl_2$ led to a free Ca^{2+} concentration of 205 μM, which saturated both binding sites in the E_1 conformation with Ca^{2+} ($K_{1/2}$ = 0.6 μM), corresponding to the reaction $E_1 + 2\ Ca^{2+} \rightarrow Ca_2E_1$. Addition of 1 mM ATP started the pumping process and, according to known rate constants of the pump cycle, the major fraction of the pumps was shifted into the state $P\text{-}E_2$ (Läuger, 1991). This partial reaction was not accompanied by a pronounced change of the fluorescence intensity at physiological pH. A further addition of a high concentration of Ca^{2+} (32 mM) was able to saturate the binding sites presented on the luminal side of the pump. The fluorescence decrease again reflected an electrogenic ion binding, $P\text{-}E_2 + 2\ Ca^{2+} \rightarrow P\text{-}E_2Ca_2$.

The latter reaction may be resolved by addition of small aliquots of $CaCl_2$ as shown in Fig. 2 *B*. The enzyme was phosphorylated by addition of 1 mM ATP in the presence of 4.5 μM free Ca^{2+} (pH 7.4). The Ca^{2+} titration was performed up to 50 mM. After correction of artifacts induced by an increase of the ionic strength at high Ca^{2+} concentrations in the electrolyte, agreement of the results obtained with 2HITC was found with those measured recently with 2BITC (Butscher et al., 1999). Experiments in Fig. 2, *A* and *B*, were performed with 2HITC, and, in Fig. 2 *C*, with 2BITC.

A pH titration experiment in state E_1 of the Ca-ATPase is presented in Fig. 2 *C*. The standard buffer (25 mM tricine, 50 mM KCl) was set to pH 8 by addition of KOH. A free Ca^{2+} concentration of 70 nM was obtained by addition of 100 μM BAPTA and 25 μM $CaCl_2$ (in addition to the residual Ca^{2+} contents of the enzyme preparation). The pH was decreased stepwise to a final pH of 5 by addition of aliquots of HCl. The pH was measured by an immersed pH microelectrode after each addition of acid.

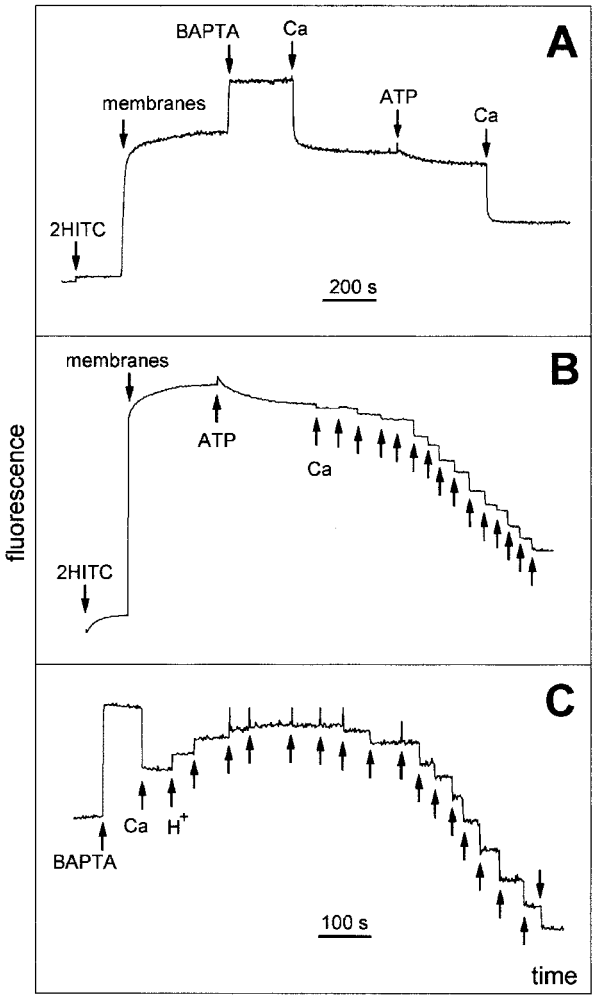

FIGURE 2 Equilibrium titration experiments with 2HITC. (*A*) The so-called standard experiment was performed in buffer (25 mM tricine, 50 mM KCl, 1 mM $MgCl_2$, pH 7.2) to which, successively, were added 200 nM 2HITC, 9 μg/ml Ca-ATPase-containing membranes, 100 μM BAPTA, 300 μM $CaCl_2$ (corresponding a free Ca^{2+} concentration of 204 μM), 1 mM ATP, and 32 mM $CaCl_2$. (*B*) Ca-titration experiment in state $P\text{-}E_2$. The experiment was started in buffer without ion chelator (pH 7.4). The free Ca^{2+} concentration was found by FURA-2 to be 4.5 μM. To transfer the enzyme into $P\text{-}E_2$, 1 mM ATP was added. The unlabeled arrows indicate where aliquots of $CaCl_2$ were added up to a final concentration of 50 mM. (*C*) pH-Titration experiment. The experiment was started like a standard experiment at pH 8.0 but with 200 nM 2BITC. In state E_1, $CaCl_2$ was added to obtain a concentration of 70 nM of free Ca^{2+}. Then, aliquots of HCl were added (*arrows*) until a final pH of 5 was reached. The pH was detected in parallel by a pH micro electrode.

In pH titration experiments in the nominal absence of Ca^{2+} (<3 nM) and in the presence of 1 mM $MgCl_2$, an increase of the fluorescence could be observed when the pH was lowered from 8 to 7 (Fig. 2 *C*). To identify the origin of this effect, a similar titration experiment was performed in the absence of Mg^{2+}. The results from both measurements are shown in Fig. 3 *A*. In the nominal absence of divalent cations, an almost monotonic fluorescence decrease was

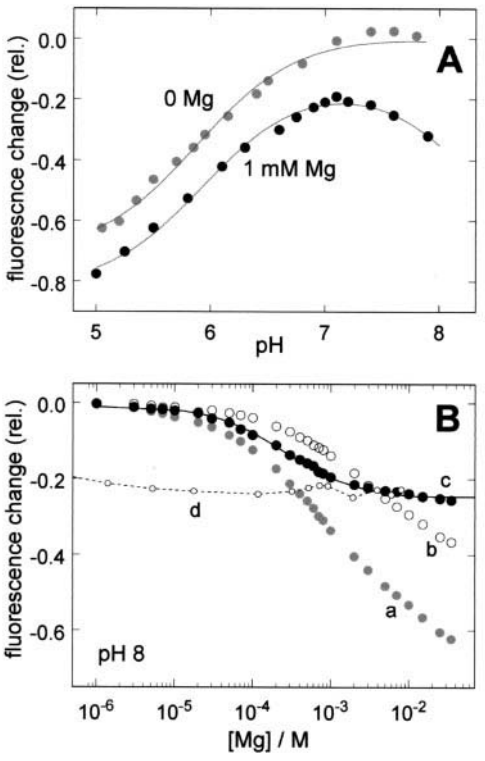

FIGURE 3 Electrogenic effects of Mg^{2+} binding to the cytoplasmic sites of the Ca-ATPase. (*A*) pH titration in the presence and absence of Mg^{2+}. The fluorescence changes were determined from experiments such as shown in Fig. 2 *C*. A significant biphasic behavior was found only in the presence of Mg^{2+} ions, which are assumed to be displaced by H^+ ions. The Ca^{2+} concentration was ~3 nM (100 μM BAPTA present). The fluorescence intensities are normalized relative to the levels before the titration was started (at about pH 8). (*B*) Effect of Mg^{2+} binding on the 2BITC fluorescence. According to the mechanism of the styryl dyes (Bühler et al., 1991; Butscher et al., 1999) the decrease of the fluorescence level is caused by an import of positive charge into the membrane dielectric. Trace *a* is the result of a titration experiment with active and trace *b* with Tharpsigargin-inactivated enzyme. The difference of both signals (*trace c*) has been assigned to the effect specific to Mg^{2+} binding. The concentration dependence could be perfectly fitted by the sum of two binding isotherms (see text). For comparison, part of a Ca^{2+} titration experiment was included to show the correspondent, saturating fluorescence level (using the same concentration axis). At pH 8, the $K_{1/2}$ value for Ca^{2+} binding was ~50 nM.

found when the pH was lowered. These data could be described by the sum of two binding isotherms (in logarithmic form)

$$F(\mathrm{pH}) = \frac{\Delta F_1}{1 + 10^{(\mathrm{pH}-\mathrm{pK}_1)}} + \frac{\Delta F_2}{1 + 10^{(\mathrm{pH}-\mathrm{pK}_2)}} + F_0, \quad (1)$$

where the ΔF_i are the respective fluorescence changes between saturating high and low pH, and F_0 is the initial fluorescence intensity before the titration experiment. The lines drawn through the experimental data in Fig. 3 *A* were fitted according to Eq. 1 with opposite effects of both isotherms on the fluorescence emission. The pK values of H^+ binding in the absence of divalent cations were found to be ~5.9 and 9. In the presence of 1 mM Mg^{2+}, they were 5.9 and 8.4. As a possible explanation for the pronounced biphasic fluorescence behavior in the presence of Mg^{2+} we assumed that the divalent cations bind in an electrogenic fashion to the ion sites and that they are displaced by protons (which carry only one elementary charge each) when pH is decreased. The reduction of the (net) positive charge within the protein dielectric is expected to lead to the observed increase in fluorescence intensity. To check directly whether Mg^{2+} binding is electrogenic, a series of Mg^{2+} titration experiments was performed in buffers of various pH. In all cases, fluorescence decreases could be observed. In Fig. 3 *B*, the fluorescence changes induced by addition of Mg^{2+} are plotted against the respective ion concentration (*curve a*). The plotted data were obtained from an experiment in a buffer of pH 8. Because it was observed that, at high Ca^{2+} concentrations (>1 mM), the divalent cations are able to quench the fluorescence intensity of the styryl dye (Butscher et al., 1999), control titration experiments were performed with enzyme-inhibited by 1 μM tharpsigargin or with membrane preparations inactivated thermally. Both treatments abolished enzymatic activity and Ca^{2+} binding completely (not shown). When the unspecific Mg^{2+}-dependent fluorescence quench, as detected in titration experiments with inactivated enzyme (*trace b*), was subtracted from the fluorescence of the active preparation (*trace a*) a fluorescence signal was obtained that was assumed to reflect the specific effect of Mg^{2+} binding to the Ca-ATPase (*trace c*). To fit the data reasonably, a sum of two binding isotherms with $K_{M,1} = 165$ μM and $K_{M,2} = 7.4$ mM was necessary (not shown). Under physiological conditions ($[Mg^{2+}] < 5$ mM), only the high affinity Mg^{2+} binding would be of interest as a reaction competing with Ca^{2+} binding. A corresponding titration experiment with Ca^{2+} (partly shown as *trace d* with the same axis as the Mg^{2+} concentration) resulted at pH 8 in a half-saturating concentration of 34 nM and in a maximal fluorescence decrease which is comparable to that of the specific Mg^{2+} effect (*trace c*).

Competition between Ca^{2+}, H^+, and Mg^{2+} ions at the cytoplasmic binding sites is demonstrated in Fig. 4. Titration experiments were performed in buffer containing 25 mM tricine, 50 mM KCl, 400 μM BAPTA, 18 μg/ml Ca-ATPase and 200 nM 2BITC, pH and Mg^{2+} concentrations as indicated. Aliquots of $CaCl_2$ were added and the actual concentrations of free Ca^{2+} were calculated. The data were fitted with the phenomenological Hill function to obtain the respective half-saturating Ca^{2+} concentrations, $K_{1/2}$. At pH 8 and 0 Mg^{2+}, a $K_{1/2}$ of 34 nM was determined (with a Hill coefficient of $n_H = 1$). At pH 7.2 (a 6.3-fold H^+ concentration) $K_{1/2}$ increased to 185 nM (a 5.6-fold increase when compared to the value at pH 8) and the Hill coefficient was increased to 1.4, suggesting a cooperativity in the binding of both Ca^{2+} ions. Addition of 1 mM $MgCl_2$ shifted $K_{1/2}$ further to a value of 364 nM, the Hill coefficient stayed

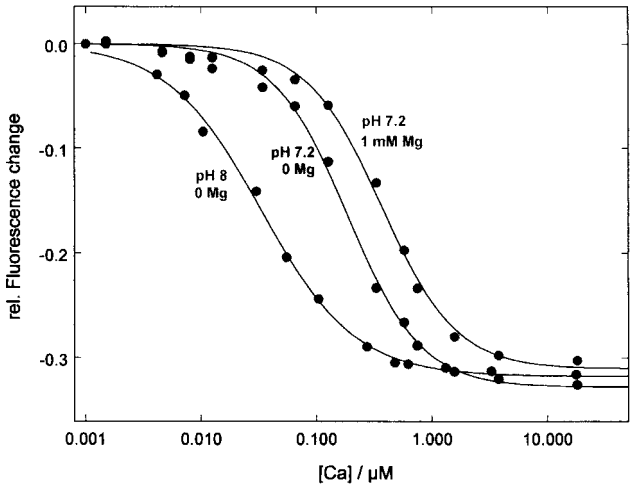

FIGURE 4 Titration of the cytoplasmic binding sites with Ca^{2+} in dependence of pH and Mg^{2+} concentration. To visualize the shift of the half-saturating Ca^{2+} concentration, the data were normalized to the respective fluorescence level before and after the additions of Ca^{2+}. The lines are drawn according to mathematical simulations of Scheme 1. The $K_{1/2}$ value derived from Hill fit to the data are 34 nM, (pH 8, 0 Mg^{2+}), 185 nM (pH 7.2, 0 Mg^{2+}) and 364 nM (pH 7.2, 1 mM Mg^{2+}).

at 1.4. A repetition of this experiment with 1 mM Mg^{2+} at pH 8 gave a $K_{1/2}$ of 130 nM and a n_H of 1.1 (not shown). These findings are clear indications that H^+ and Mg^{2+} ions affect competitively Ca^{2+} binding.

Other control experiments to clarify the origin of the biphasic behavior in the pH titration experiment were titrations in the absence of Mg^{2+} and in the presence of low Ca^{2+} concentrations (Fig. 5, *b* and *c*). In the presence of 195 nM Ca^{2+}, pH dependence of the fluorescence intensity was comparable to that detected at 1 mM Mg^{2+} (Fig. 5, *c* and *e*). From this observation, we concluded that Mg^{2+} ions are able to bind to the cytoplasmic Ca^{2+} binding sites (with a significantly lower affinity when compared with Ca^{2+} (165 μM for Mg^{2+} versus 34 nM for Ca^{2+}), and that protons are able to compete in the binding sites with both divalent ions.

To investigate the competition between these ions, numerous pH titrations were performed at various Ca^{2+} and Mg^{2+} concentrations. A selection of measurements is shown in Fig. 5. In these experiments, the reference fluorescence intensity, F_0, was obtained for all experiments from the stationary level, which was obtained after 200 nM 2BITC and 18 μg/ml Ca-ATPase were incubated in buffer containing 25 mM tricine, 50 mM KCl, 100 μM BAPTA at an initial pH in the range of 7.9 $\pm$ 0.1. Subsequently, $MgCl_2$ and $CaCl_2$ were added to the final concentrations as indicated in Fig. 5, before the pH titration was performed. After each addition of HCl the actual pH was measured by an immersed pH micro electrode. It can be seen that the biphasic fluorescence behavior was always observed when divalent cations, Ca^{2+} or Mg^{2+}, were present. In the virtual absence of Ca^{2+} ($\sim$3 nM), addition of low concentrations of Mg^{2+} ($\lesssim$100 μM) had hardly any effect on the pH-dependent fluorescence intensity and only a slight indication of a beginning biphasic behavior is visible (not shown), and the fluorescence levels below pH 7.5 are in full agreement with that of the experiment in the absence of divalent cations (*panel a*), significant changes became obvious at Mg^{2+} concentrations of 500 μM and higher (*panels d–f*). In contrast, the presence of 100 μM Ca^{2+} (and 0 Mg^{2+}) reduced the fluorescence changes to one third (*panel i*), a repetition of this experiment with a further addition of 1 mM Mg^{2+} induced no further changes (not shown). All these findings point to a competition of all three ions participating in these experiments (see Discussion).

Ion binding to the luminal ion binding sites

To perform pH and Ca^{2+} titration experiments in the P-E_2 state of the Ca-ATPase, 200 nM 2HITC and SR membranes (18 μg/ml protein) were equilibrated in buffer containing 25 mM tricine, 50 mM KCl, pH 7.4. In the absence of a chelator, the free Ca^{2+} concentration was found to be $\sim$5 μM. Therefore, the addition of 1 mM ATP transferred the ion pumps into states of P-E_2. Subsequently, $CaCl_2$ was added from concentrated stock solutions to obtain final concentrations between 50 μM and 20 mM, which were able to equilibrate between inside the SR vesicles and the buffer before the fluorescence intensity was measured. Then and after each subsequent addition of HCl, the pH was measured by an immersed pH micro electrode. The fluorescence intensity levels were normalized to the steady-state level after the initial addition of ATP. Fluorescence levels of a continuous Ca^{2+} titration with 2HITC at a constant pH of 7.4 were compared with corresponding levels extracted from a number of pH titration experiments at defined Ca^{2+} concentrations, and no significant differences were found (Fig. 6). This is also true when these data are compared with a recently published measurement performed with another styryl dye, 2BITC. The line in Fig. 6 represents the sum of two binding isotherms with equilibrium dissociation constants of K_1 = 2 mM and K_2 = 5 μM as reported recently (Butscher et al., 1999). The Ca^{2+} titration experiments were also performed in buffer of the same composition but at pH 5 (data not shown). Ca^{2+} titration experiments in the P-E_2 conformation were performed also in the presence of 10 μM A23187 to increase the permeability of the SR membranes for Ca^{2+}. These controls did not produce significant alterations of the equilibrium dissociation constants (not shown). A selection of the pH titration experiments is shown in Fig. 7. In the state P-E_2, no biphasic pH dependence was detected, but a monotonic decrease of the 2HITC (or 2BITC) fluorescence intensity with increasing H^+ concentration. Although the initial fluorescence level depended on the amount of Ca^{2+} present (Fig. 6), the titration curves merged at the lowest pH measured ($\sim$pH 5). A phenomenological description of these data with a Hill function led to Hill

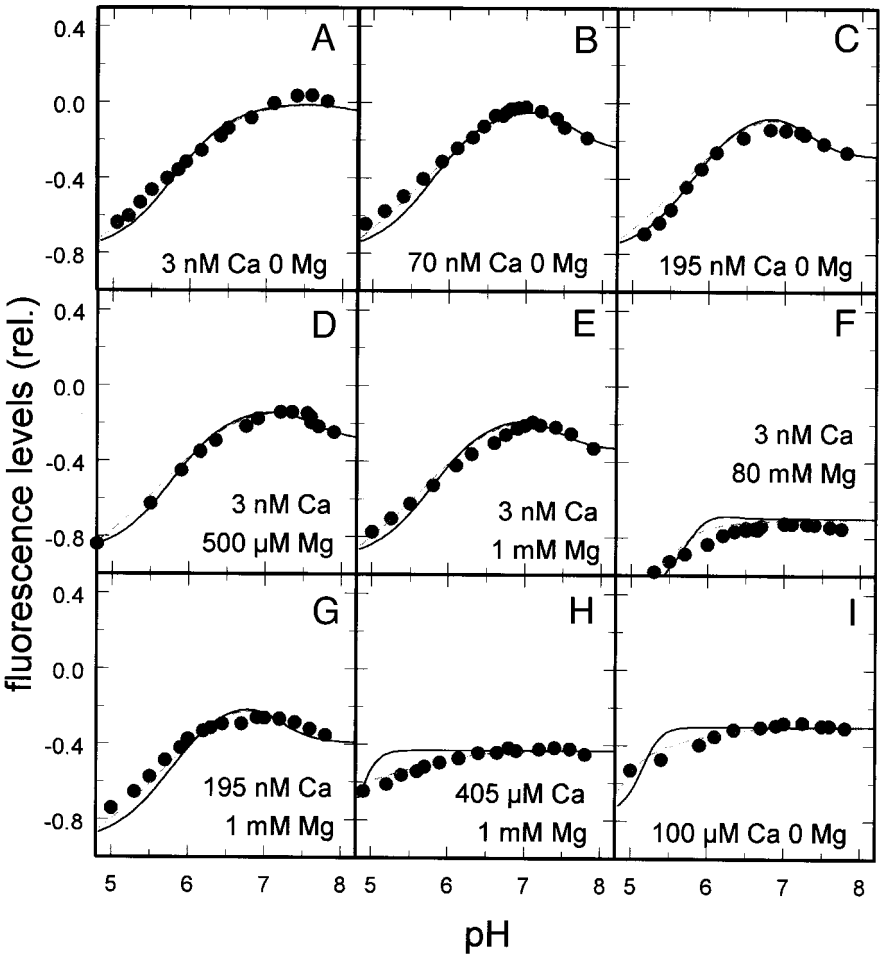

FIGURE 5 Effect of Ca^{2+} and Mg^{2+} ions on proton binding in the E_1 conformation of the Ca-ATPase. All experiments were started in buffer containing 25 mM tricine, 50 mM KCl, 100 μM BAPTA, and an initial pH of 7.8–8.0. After $CaCl_2$ and $MgCl_2$ were added to reach the indicated concentration of free cations, the pH titration was performed by additions of appropriate aliquots of HCl. The fluorescence intensities were normalized with respect to the level before the addition of divalent ions. The solid line represents the results of a mathematical simulation of Scheme 1, the dashed lines were calculated from a model that includes additional allosteric binding of an H^+ ion (see text).

coefficient in the order of 0.8, which is an indication of a mechanism more complex than a simple binding of a single H^+ ion.

Mg^{2+} titration experiments in state P-E_2 could not be performed with the membrane preparations available, because the (inevitable) simultaneous presence of Mg^{2+} on the cytoplasmic side in concentrations above 1 mM led to increasing competition with the low Ca^{2+} concentration at the cytoplasmic sites and prevented at least partially the ATP-driven turnover into the P-E_2 states, so that the enzyme was virtually trapped in its E_1 conformation and finally the Mg^{2+} titration in E_1 was reproduced instead (not shown).

DISCUSSION

It is generally accepted that, in the Ca-ATPase, both ions are moved across the SR membrane by a ping-pong mechanism, which is common for all known P-type ATPases (Läuger, 1991; Andersen and Vilsen, 1995), and the transported Ca^{2+} and H^+ ions bind probably to the same or closely related structures inside the protein. Although Ca^{2+} has a six-fold coordination in the binding site (Toyoshima et al., 2000), H^+ ions are able to bind to a single negatively charged side chain without further coordination if they are not transported in the form of a hydronium ion. Mg^{2+} ions present in the cytoplasm are an essential cofactor as Mg·ATP. However, as a similar sized divalent cation, Mg^{2+} is able to compete as a free ion with Ca^{2+}, as can be seen from Figs. 4 and 5, although no transport of Mg^{2+} (or phosphatase activity in the presence of Mg^{2+} alone) by the SR Ca-ATPase was detected.

As shown recently (Butscher et al., 1999), all ion binding and release steps of the SR Ca-ATPase affect the fluorescence levels of styryl dyes. According to the published mechanism of the styryl dyes, such as 2BITC, 2HITC, or RH421, the dyes detect, preferentially, charges that are

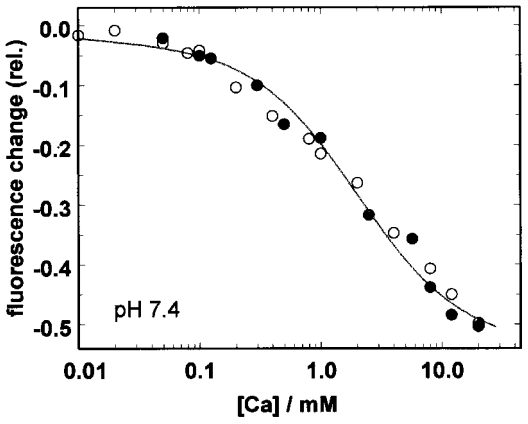

FIGURE 6 Comparison of Ca^{2+}-titration experiments in state P-E_2 of the Ca-ATPase. Data points result from experiments performed with the styryl dye 2HITC. The line represents the fit through the data of an experiment performed with 2BITC. It is a sum of two binding isotherms with equilibrium dissociation constants of $K_1 = 5\ \mu M$ and $K_2 = 1.8$ mM (Butscher et al., 1999). The open circles are taken from a measurement in which successively aliquots of $CaCl_2$ solutions were added. The solid circles represent the starting points of pH titration experiments as shown in Fig. 5 at various initial Ca^{2+} concentrations. All three experiments fit well together.

imported into or exported from the membrane/protein dielectric (Bühler et al., 1991; M. Pedersen, M. Roudna, S. Beutner, M. Birmes, B. Reiters, H.-D. Martin, and H.-J. Apell, submitted for publication). When binding of each cation species, Ca^{2+}, Mg^{2+}, and H^+, is investigated in the (virtual) absence of the others, it was found that the fluorescence decreased monotonically with increasing ion concentration. This indicates that the amount of positive charge inside the pump was increased successively. The biphasic behavior found in pH titration experiments in the E_1 state of the protein in the presence of Mg^{2+} ions or low concentration of Ca^{2+} ions (Fig. 5) can be understood by the mechanism that all or part of the divalent cations in the binding sites are replaced by the monovalent H^+, which has a smaller effect on the electrogenic fluorescence changes of the electrochromic dyes.

Analysis of the ion binding kinetics in E_1

At a pH of 7.4 and in the presence of 1 mM Mg^{2+}, the fluorescence decrease induced by Ca^{2+} binding to the cytoplasmic sites can be fitted either with the phenomenological Hill equation ($K_{1/2} = 5.9 \cdot 10^{-7}$ M, $n_H = 2$) or simulated with a reaction scheme according to the known binding stoichiometry, $E_1 \rightleftarrows CaE_1 \rightleftarrows Ca_2E_1$. The latter scheme is defined by two equilibrium dissociation constants that were determined from least-square fits, which resulted in the apparent values of $K_{1,Ca} = 0.6 \cdot 10^{-5}$ M and $K_{2,Ca} = 0.62 \cdot 10^{-7}$ M (Butscher et al., 1999). It is remarkable that binding of the first Ca^{2+} ion occurred with the lower affinity than the second. This fact was observed earlier (Inesi and de Meis, 1989) and interpreted that the second site becomes available only after the first is occupied (Inesi et al., 1990; Menguy et al., 1998). Such an inverted binding affinity was also found also in case of the binding of the second and third Na^+ ion to the E_1 state of the Na,K-ATPase, and explained by the fact that the site with the higher affinity is accessible only after the site with the lower affinity is occupied by a Na^+ ion (Schneeberger and Apell, 2001). However, this inverted order of the binding affinity under physiological conditions may be explained also as an apparent effect due to a competition between Ca^{2+} and H^+ and Mg^{2+} at the binding sites as discussed in the following.

To reproduce the titration experiments with Ca^{2+}, Mg^{2+}, H^+ and all tested mixtures of the three ion species, we started with the reaction scheme (Scheme 1), which describes a linear competition between all three kinds of ions. To simulate the equilibrium titration experiments, the system of nine coupled linear equations, which represent Scheme 1, was solved, and the population of the enzyme states were obtained as functions of the ion concentrations and of the equilibrium dissociation constants, K_i, as shown in the Appendix. All titration experiments performed with respect to ion binding and competition in state E_1 (Figs. 3–5) were fitted with the final analytical function of the fluorescence intensity in Eq. A29, $F([H^+], [Ca^{2+}], [Mg^{2+}])$, by a single set of K_i. To reproduce all presented experiments, the equilibrium dissociation constants of Scheme 1 were determined to be for Ca^{2+} $K_1 = 4 \cdot 10^{-8}$ M and $K_2 = 5 \cdot 10^{-8}$ M, for Mg^{2+} $K_3 = 5 \cdot 10^{-5}$ M and $K_4 = 1 \cdot 10^{-3}$ M, and for H^+ $K_5 = 10^{-8}$ M and $K_6 = 10^{-8}$ M, $K_7 = 10^{-6}$ M and $K_8 = 10^{-5}$ M. The solid lines in Fig. 5 represent the results of the simulations of Scheme 1 with these parameters. At pH > 6, the experimental results were reproduced to our satisfaction. However, it turned out that this reaction scheme produced significant deviations in the case of experiments at a pH < 6 and at unphysiolocially high concentrations of Ca^{2+} or Mg^{2+} (Fig. 5, *f–i*). Possible explanations are discussed below. To account for the decrease of the fluorescence intensity by high Mg^{2+} concentrations ($>500\ \mu M$), which were caused by an unspecific quench of the styryl fluorescence as shown in Fig. 3 *B* (*trace b*), the calculated fluorescence intensities were corrected by the respective fluorescence offset at the corresponding Mg^{2+} concentration.

Under the assumption that Scheme 1 is a fair representation of the interaction of cations with the cytoplasmic binding sites, the equilibrium dissociation constants obtained for both Ca^{2+} sites are equal, $K_1 = 40$ nM and $K_2 = 50$ nM. These "primary" constants are significantly smaller than the "operative" constants obtained under physiological buffer conditions (about 360 nM, Fig. 4). The finding that $K_1 \approx K_2$ is important with respect to mechanistic implications. If both binding sites were accessible simultaneously, then a statistical effect would occur, which is caused by the

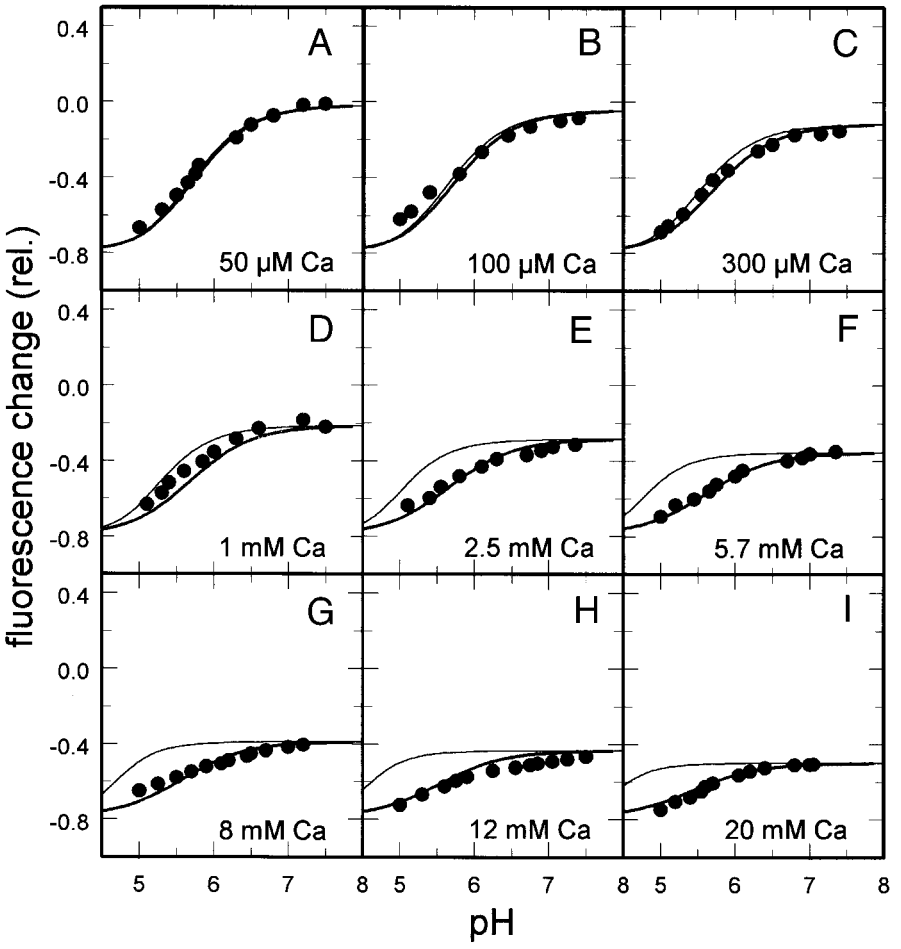

FIGURE 7 Effect of Ca^{2+} ions on proton binding in the P-E_2 conformation of the Ca-ATPase. In all experiments, the pH titration was started in buffer containing 25 mM tricine, 50 mM KCl, 1 mM Mg^{2+}, 1 mM ATP, and the indicated concentration of Ca^{2+}. After each addition of HCl, the actual pH was measured by a pH micro electrode. The hairlines represent the results of numerical simulations of a linear competition model between Ca^{2+} and H^+ (Scheme 2a), the bold lines represent the results of numerical simulations of a branched competition model between Ca^{2+} and H^+ (Scheme 2b).

fact that the first ion to bind and the first ion to dissociate each have the choice between two sites. This would account for a factor of $K_2/K_1 = 4$ between both equilibrium dissociation constants. Because this difference was not found, it has to be assumed that, indeed, a defined access order exists in binding (and release) of the Ca^{2+} ions on the cytoplasmic side. This is in agreement with the well-documented binding studies of Inesi (1987). The apparent lower affinity of the first Ca^{2+} site in buffer containing 1 mM Mg^{2+} (or more) is the consequence of a competition between Ca^{2+} and Mg^{2+} at the first site. Competition between Ca^{2+} and Mg^{2+} at the second site is significantly lower due to the five orders in magnitude difference between the affinities (Ca^{2+}: $K_2 = 5 \cdot 10^{-8}$ M, Mg^{2+}: $K_4 = 1 \cdot 10^{-3}$ M). Therefore, the proposed reaction scheme and the equilibrium constants determined from the presented experiments are in good agreement with known physiological properties of Ca^{2+} binding to the SR Ca-ATPase.

$$\begin{array}{ccccccccccccc} & & & & & & & & E_1Mg_2 & & & & \\ & & & & & & & & \Updownarrow K_4 & & & & \\ & & & & & & & & E_1Mg & & & & \\ & & & & & & & & \Updownarrow K_3 & & & & \\ E_1H_4 & \underset{K_8}{\rightleftarrows} & E_1H_3 & \underset{K_7}{\rightleftarrows} & E_1H_2 & \underset{K_6}{\rightleftarrows} & E_1H & \underset{K_5}{\rightleftarrows} & E_1 & \underset{K_1}{\rightleftarrows} & E_1Ca & \underset{K_2}{\rightleftarrows} & E_1Ca_2 \end{array}$$

SCHEME 1

Mg^{2+} binding at pH 8 and in the absence of Ca^{2+} produced data that can be described phenomenologically by a Hill function ($K_{1/2} = 2.1 \cdot 10^{-4}$ M, $n_H = 0.68$). The assumption that Mg^{2+} could enter the Ca^{2+} binding sites led to the proposal of the reaction scheme, $E_1 \rightleftarrows MgE_1 \rightleftarrows Mg_2E_1$, which allowed a simulation of the experimental data as shown in Fig. 3 *B* (with $K_3 \equiv K_{1,Mg} = 5 \cdot 10^{-5}$ M and $K_4 \equiv K_{2,Mg} = 1 \cdot 10^{-3}$ M). With these parameters, it could be shown (see above) that, under physiological conditions (about 1 mM Mg^{2+}) an antagonizing effect of Mg^{2+} on the

Ca^{2+} binding will occur. This is more obvious in the data presented in Fig. 4, where the apparent half-saturating concentration of Ca^{2+} was significantly shifted as a consequence of an increased concentration of H^+ and of Mg^{2+} ions. This competition and the electrogenicity of Mg^{2+} binding indicate that the sites are the ion sites and not the specific Mg^{2+} site that has to be occupied for the use of ATP.

H^+ binding in the absence of divalent cations was performed in the pH range between 8 and 5 and could be approximated with a single binding isotherm with a pK ~ 5.8 (Fig. 5 *A*). In addition, and on the basis of the observation of Yu et al. (1994) simulations were performed with reaction schemes that bind up to 4 H^+ ions, $E_1 \rightleftarrows HE_1 \rightleftarrows H_2E_1 \rightleftarrows H_3E_1 \rightleftarrows H_4E_1$. Although the differences between the fits of the data with a binding isotherm and with mathematical simulations of this more complex reaction scheme were not significant in the case of a simple pH titration experiment, the pH titration experiments in the presence of various concentrations of Ca^{2+} and Mg^{2+} led to a discrimination among at least three different sites (see below).

To obtain ideas on the mechanism, which caused the pH dependence of the fluorescence (Fig. 5, *f–i*) that was not explained by the results obtained from Scheme 1, we introduced an additional binding of an H^+ to an allosteric binding site that affects the binding affinity of the sites for Ca^{2+} or Mg^{2+} at low pH. In an unphysiologically low pH range (<6), it was also found experimentally that the enzymatic activity was inhibited (data not shown). The observed, additional effect on the fluorescence intensity (Fig. 5) could occur, e.g., by protonation of a carboxyl side chain of an amino acid, either in the ion binding site, where it would affect ion binding directly, or in the access pathway for the ions to the binding sites, where it would reduce the local concentration of Ca^{2+} or Mg^{2+} ions due to a Gouy–Chapman effect. Information on the molecular mechanism is not available on the basis of the investigations performed so far. However, the introduction of an allosteric H^+ binding, that affects protein states that have Ca^{2+} or Mg^{2+} bound, provided a better simulation of the experimental data (Fig. 5, *dashed lines*) in the low pH range (<6.5). The pK of the additional H^+ binding reaction was set to 5.5 to result in an optimal fit to the data. In a buffer environment of physiological pH (>7), however, less than 3% of the proposed allosteric site would be protonated. Therefore, it can be concluded that this process is only an unphysiological side track in the reaction scheme and is not necessary to describe the ion transport processes as they occur in muscle cells.

In summary, it can be concluded that Scheme 1 is an appropriate description of the reaction mechanism relevant for ion binding to and competition at the cytoplasmic sites of the SR Ca-ATPase. It is remarkable that all experiments performed can be described without a branched reaction scheme, in contrast to the experimental findings on the luminal side of the pump (see below). This could be a hint on structural constraints with respect to ion binding in E_1. Under physiological conditions, such as pH 7.2 and 1 mM Mg^{2+}, the competition between Ca^{2+} as primary substrate on one hand and H^+ and Mg^{2+} on the other reduces the steady-state occupation with two Ca^{2+} ions significantly, as is visible in Fig. 4. How relevant this reduction is for the cycling of the pump under turnover conditions will be investigated in forthcoming work on time-resolved kinetics.

The ATP-induced transitions from E_1 into the states of P-E_2 were found to produce only a small fluorescence change and to have complex time course, as can be seen in Fig. 2, *A* and *B*. Under the condition of this experiment (4.5 μM Ca^{2+} and 1 mM Mg^{2+}), the partial reaction is decelerated by almost a factor of 10 when compared to the turnover rate, probably due to a dynamic inhibition by H^+ and Mg^{2+} ions present in the buffer. A detailed time-resolved investigation of this partial reaction is under progress. The steady-state fluorescence level after addition of ATP was found to be pH dependent (Butscher et al., 1999). At pH 7.2, the small fluorescence change indicates that the amount of (net) charge within the protein dielectric did not change significantly between the steady states before and after the ATP-induced conformation transition. Two processes may contribute to this finding: an immediate H^+ binding in P-E_2 after release of Ca^{2+} to the luminal side, and a conformation-dependent shift of charged residues of the binding sites closer to the luminal surface of the protein, perhaps into a water-filled vestibule.

Analysis of the ion binding kinetics in P-E_2

Corresponding to the observations in the E_1 states, it was found that Ca^{2+} and H^+ ions compete also for the same sites in the P-E_2 states of the Ca-ATPase (Butscher et al., 1999; Forge et al., 1993; Yu et al., 1994). Experimentally, it was possible to study the interaction of Ca^{2+} and H^+. Effects of Mg^{2+} at the luminal sites, however, could not be detected, because, after addition of Mg^{2+} to the SR membrane preparations, the ions were always present on both sides of the membrane. Therefore, when in the presence of low Ca^{2+} concentrations, the Mg^{2+} concentrations were increased above 1 mM, its binding of Mg^{2+} to the enzyme in the E_1 conformation prevented, at least partially, phosphorylation of the enzyme by ATP and its turnover into P-E_2 states, and disabled, in this way, binding of Mg^{2+} to the luminal sites of the pump.

In the analysis of the mutual effects of Ca^{2+} and H^+ on binding in the P-E_2 states (Fig. 7) the data were simulated in a first step by the mathematical representation of a simple linear reaction scheme (Scheme 2a). This scheme describes competitive binding to the same sites. However, in contrast to the results of the cytoplasmic ion-binding reactions, it produced no satisfying Ca^{2+} and pH concentration dependence of the fluorescence amplitude (Fig. 7, *hairlines*), and the apparent pK of the pH titration as a function of the Ca^{2+} concentration was in

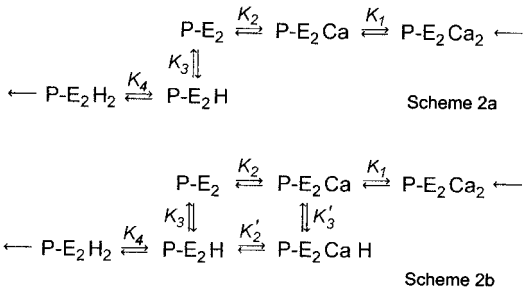

SCHEME 2

clear disagreement with the experiments (Fig. 8 *A*, *dashed line*). When the equilibrium dissociation constants were chosen to fit the data in the presence of 50 μM Ca^{2+} (K_1 = 25 mM, K_2 = 0.4 mM, $K_3 = 2 \cdot 10^{-6}$ M (i.e., pK 5.7), $K_4 = 10^{-5}$ M (i.e., pK 5)), at Ca^{2+} concentrations above 1 mM, no fit was obtained (Fig. 7, *hairlines*). Therefore, in a second step, the reaction scheme was modified, and a mixed state, P-E_2HCa, was introduced (Scheme 2b). With this additional state, even under the simplifying assumption that the high-affinity Ca^{2+} binding is independent of the presence of a bound H^+ ion, i.e., $K_2 = K_2' = 0.4$ mM, and that binding of the first H^+ is independent of the presence of the high-affinity Ca^{2+}, i.e., $K_3 = K_3' = 2 \cdot 10^{-6}$ M (pK 5.7), an almost perfect fit of the experimental data was obtained, as can be seen in Figs. 7 and 8, without changing the equilibrium dissociation constants from Scheme 2a. The insignificant dependence of the apparent pK on the Ca^{2+} concentration, as shown in Fig. 8 *A*, indicates that H^+ binding indeed is almost unaffected by the presence of Ca^{2+} up to a concentration of 10 mM. In contrast, it was found that low-affinity Ca^{2+} binding in P-E_2 was strongly affected by pH, but not high-affinity binding (Fig. 8 *B*). The pH dependence of the low-affinity Ca^{2+} binding can be reproduced by binding of an H^+ ion to a negatively charged side group with an apparent pK of 7.2, which, in turn, reduces significantly the affinity for Ca^{2+} by about a factor of 3 ($K_{1/2}$(pH $<$ 5) $\sim$ 15 mM, $K_{1/2}$(pH $>$ 9) $\sim$ 5 mM). This observation led to the suggestion that the H^+ ions may be able to protonate negatively charged side chains of amino acids at the low-affinity Ca^{2+} binding site and leave behind a water molecule, of which about 30 were found in the transmembrane region of the Ca-ATPase (Toyoshima et al., 2000). Such a binding process would produce no steric obstacle for binding or release of the high-affinity Ca^{2+} ion, which obviously was not affected by the pH. Vice versa, a Ca^{2+} ion bound to the high-affinity site did not affect H^+ binding to the low-affinity Ca^{2+} site. Such a mixed state has been already proposed by Yu et al. (1994).

In the P-E_2 conformation, both Ca^{2+} binding sites have significantly different equilibrium dissociation constants, which are 0.4 and 25 mM, as was obtained by a simulation of the experimental data with Scheme 2b. This observation cannot be explained solely by different electrostatic interactions of the first and second Ca^{2+} with the protein matrix

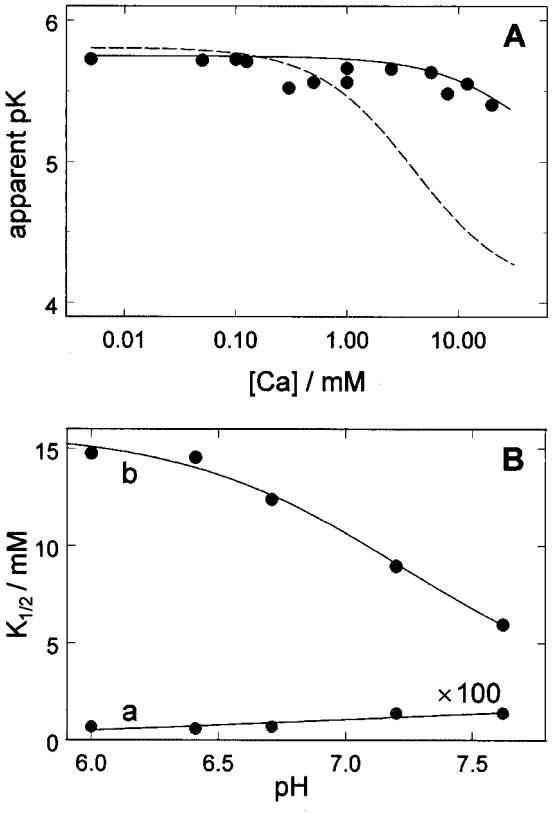

FIGURE 8 Mutual dependence of Ca^{2+} and H^+ ions on ion binding to the luminal sites of the Ca-ATPase. (*A*) Dependence of the apparent pK of proton binding in the P-E_2 conformation. The circles were determined from experiments, such as shown in Fig. 7, by fitting binding isotherms to data points. The lines were obtained from the mathematical solution of assumed partial reactions of Scheme 2a (*dashed line*) and Scheme 2b (*solid line*). (*B*) pH dependence of Ca^{2+} binding in state P-E_2. Binding of the two Ca^{2+} ions could be discriminated as high-affinity and low-affinity binding (Butscher et al., 1999). The equilibrium dissociation constant of the high-affinity binding (*trace a*) was pH independent, $K_{1/2}$ = (9 $\pm$ 1.6) μM. The low-affinity binding was simulated according to the Henderson–Hasselbalch equation under the assumption of an H^+ that binds to a negatively charged site with an apparent pK of 7.2 (*trace b*).

or by the statistical effect that the first Ca^{2+} ion to bind or to dissociate has two choices (which would produce a factor of $K_2/K_1 = 4$). The observation that H^+ binding affects low affinity Ca^{2+} binding in a competitive way but not high affinity Ca^{2+} binding, leads to the suggestion that both sites have to be significantly different in P-E_2. The recently published structure of the Ca^{2+}-binding sites, I and II of the crystal structure, revealed that five carboxyl side chains are involved at each site, one of them (Asp-800) coordinates both Ca^{2+} ions (Toyoshima et al., 2000). Therefore, on the evidence available at the moment it is not possible to assign the high- and low-affinity sites to the introduced sites I and II. In addition, the transition from the E_1 conformation into the P-E_2 conformation is accompanied by a dramatic decrease of Ca^{2+} binding affinity from ~40 nM (in Scheme 1)

to ~25 mM and 0.4 mM (in Scheme 2b). These changes have to have a counterpart in structural rearrangements.

The pH dependence of the fluorescence signals in state E_1 could be reproduced best with the assumption that, at low pH values, up to four H^+ are bound inside the transmembrane region of the ion pump. Two of the H^+ are bound but not transported across the SR membrane. This would be in agreement with an earlier proposed mechanism (Yu et al., 1994) and would not be in contradiction to the published structural features.

In the E_1 conformation, it was found that the ion binding sites are positioned approximately in the center of the transmembrane region of the protein (Toyoshima et al., 2000). If we assume that, due to the nature of the binding sites, their shift into another position is small when the protein undergoes the transition into state P-E_2, the question arises why the fluorescence levels of both states, Ca_2E_1 and P-E_2Ca_2, are significantly different (Fig. 2 *A*). If the sites are not significantly moved, one would expect that the states Ca_2E_1, $(Ca_2)E_1$-P, and P-E_2Ca_2 have to have the same specific fluorescence signal according to the known mechanism of the dyes. A similar observation was made in the case of the Na,K-ATPase loaded with 3 Na^+ ions (Heyse et al., 1994). A release of the two Ca^{2+} ions to the luminal aqueous phase should therefore produce a fluorescence increase. The absence of such a fluorescence response can be accepted as basis for a proposal that, during the conformational change, $(Ca_2)E_1$-P $\rightarrow$ P-E_2Ca_2, the binding sites are moved either closer to the luminal interface or a wide, water-filled vestibule is formed. These structural ideas will come to test when high-resolution structural information of the P-E_2 conformation becomes available and, possibly, with time-resolved kinetic experiments which are planned.

APPENDIX

The mathematical representation of Scheme 1 is

$$[E_1][Ca^{2+}] = K_1 \cdot [E_1Ca] \quad (A1)$$

$$[E_1Ca][Ca^{2+}] = K_2 \cdot [E_1Ca_2] \quad (A2)$$

$$[E_1][Mg^{2+}] = K_3 \cdot [E_1Mg] \quad (A3)$$

$$[E_1Mg][Mg^{2+}] = K_4 \cdot [E_1Mg_2] \quad (A4)$$

$$[E_1][H^+] = K_5 \cdot [E_1H] \quad (A5)$$

$$[E_1H][H^+] = K_6 \cdot [E_1H_2] \quad (A6)$$

$$[E_1H_2][H^+] = K_7 \cdot [E_1H_3] \quad (A7)$$

$$[E_1H_3][H^+] = K_8 \cdot [E_1H_4] \quad (A8)$$

In addition, the normalization condition holds:

$$[E_1] + [E_1Ca] + [E_1Ca_2] + [E_1Mg] + [E_1Mg_2] + [E_1H] + [E_1H_2] + [E_1H_3] + [E_1H_4] = 1 \quad (A9)$$

The solution of this equation system is

$$[E_1] = x_1/D \quad (A10)$$

$$[E_1Ca] = x_2/D \quad (A11)$$

$$[E_1Ca_2] = x_3/D \quad (A12)$$

$$[E_1Mg] = x_4/D \quad (A13)$$

$$[E_1Mg_2] = x_5/D \quad (A14)$$

$$[E_1H] = x_6/D \quad (A15)$$

$$[E_1H_2] = x_7/D \quad (A16)$$

$$[E_1H_3] = x_8/D \quad (A17)$$

$$[E_1H_4] = x_9/D \quad (A18)$$

where

$$x_1 = K_1 \cdot K_2 \cdot K_3 \cdot K_4 \cdot K_5 \cdot K_6 \cdot K_7 \cdot K_8 \quad (A19)$$

$$x_2 = [Ca^{2+}] \cdot K_2 \cdot K_3 \cdot K_4 \cdot K_5 \cdot K_6 \cdot K_7 \cdot K_8 \quad (A20)$$

$$x_3 = [Ca^{2+}]^2 \cdot K_3 \cdot K_4 \cdot K_5 \cdot K_6 \cdot K_7 \cdot K_8 \quad (A21)$$

$$x_4 = K_1 \cdot K_2 \cdot [Mg^{2+}] \cdot K_4 \cdot K_5 \cdot K_6 \cdot K_7 \cdot K_8 \quad (A22)$$

$$x_5 = K_1 \cdot K_2 \cdot [Mg^{2+}]^2 \cdot K_5 \cdot K_6 \cdot K_7 \cdot K_8 \quad (A23)$$

$$x_6 = K_1 \cdot K_2 \cdot K_3 \cdot K_4 \cdot [H^+] \cdot K_6 \cdot K_7 \cdot K_8 \quad (A24)$$

$$x_7 = K_1 \cdot K_2 \cdot K_3 \cdot K_4 \cdot [H^+]^2 \cdot K_7 \cdot K_8 \quad (A25)$$

$$x_8 = K_1 \cdot K_2 \cdot K_3 \cdot K_4 \cdot [H^+]^3 \cdot K_8 \quad (A26)$$

$$x_9 = K_1 \cdot K_2 \cdot K_3 \cdot K_4 \cdot [H^+]^4 \quad (A27)$$

$$D = x_1 + x_2 + x_3 + x_4 + x_5 + x_6 + x_7 + x_8 + x_9 \quad (A28)$$

From the normalized concentration, if, in each state in the reaction scheme $[E_x]$, the fluorescence intensity as measured in the experiments was calculated according to

$$F([H^+], [Ca^{2+}], [Mg^{2+}]) = f_1 \cdot [E_1] + f_2 \cdot [E_1Ca] + f_3 \cdot [E_1Ca_2] + f_4 \cdot [E_1Mg] + f_5 \cdot [E_1Mg_2] + f_6 \cdot [E_1H] + f_7 \cdot [E_1H_2] + f_8 \cdot [E_1H_3] + f_9 \cdot [E_1H_4]. \quad (A29)$$

The specific fluorescence levels, f_i ($i = 1, \ldots, 9$), depend on the styryl dye used, and they were obtained experimentally for 2BITC to be $f_1 = 0$ (by definition), $f_2 = -0.28, f_3 = -0.3, f_4 = -0.17, f_5 = -0.25, f_6 = 0, f_7 = 0, f_8 = -0.5, f_9 = -0.9$.

We thank M. Roudna for excellent technical assistance, Prof. Dr. H.-D. Martin and his collaborators, University of Düsseldorf, Germany, for providing the styryl dyes, and Dr. R. J. Clarke for critical reading of the manuscript.

This work was financially supported by the Deutsche Forschungsgemeinschaft (Ap 45/4).

REFERENCES

Andersen, J. P., and B. Vilsen. 1995. Structure–function relationships of cation translocation by Ca^{2+}- and Na^+,K^+-ATPases studied by site-directed mutagenesis. *FEBS Lett.* 359:101–106.

Apell, H.-J., and B. Bersch. 1987. Oxonol VI as an optical indicator for membrane potentials in lipid vesicles. *Biochim. Biophys. Acta.* 903: 480–494.

Apell, H.-J., M. Roudna, J. E. Corrie, and D. R. Trentham. 1996. Kinetics of the phosphorylation of Na,K-ATPase by inorganic phosphate detected by a fluorescence method. *Biochemistry.* 35:10922–10930.

Birmes, M. 1995. Neuartige membranpotentialsensitive Fluoreszenzfarbstoffe mit Styrylpyridiniumchromophor. PhD thesis. University of Düsseldorf, Germany. pp. 1–248.

Butscher, C., M. Roudna, and H.-J. Apell. 1999. Electrogenic partial reactions of the SR-Ca-ATPase investigated by a fluorescence method. *J. Membr. Biol.* 168:169–181.

Bühler, R., W. Stürmer, H.-J. Apell, and P. Läuger. 1991. Charge translocation by the Na,K-pump: I. Kinetics of local field changes studied by time-resolved fluorescence measurements. *J. Membr. Biol.* 121: 141–161.

Clarke, R. J., D. J. Kane, H.-J. Apell, M. Roudna, and E. Bamberg. 1998. Kinetics of Na^+-dependent conformational changes of rabbit kidney Na^+,K^+-ATPase. *Biophys. J.* 75:1340–1353.

Forge, V., E. Mintz, D. Canet, and F. Guillain. 1995. Lumenal Ca^{2+} dissociation from the phosphorylated Ca^{2+}-ATPase of the sarcoplasmic reticulum is sequential. *J. Biol. Chem.* 270:18271–18276.

Forge, V., E. Mintz, and F. Guillain. 1993. Ca^{2+} binding to sarcoplasmic reticulum ATPase revisited. I. Mechanism of affinity and cooperativity modulation by H^+ and Mg^{2+}. *J. Biol. Chem.* 268:10953–10960.

Franzini-Armstrong, C., and D. G. Ferguson. 1985. Density and disposition of Ca^{2+}-ATPase in sarcoplasmic reticulum membrane as determined by shadowing techniques. *Biophys. J.* 48:607–615.

Heilmann, C., D. Brdiczka, E. Nickel, and D. Pette. 1977. ATPase activities, Ca^{2+} transport and phosphoprotein formation in sarcoplasmic reticulum subfractions of fast and slow rabbit muscles. *Eur. J. Biochem.* 81:211–222.

Heyse, S., I. Wuddel, H.-J. Apell, and W. Stürmer. 1994. Partial reactions of the Na,K-ATPase: determination of rate constants. *J. Gen. Physiol.* 104:197–240.

Inesi, G. 1987. Sequential mechanism of calcium binding and translocation in sarcoplasmic reticulum adenosine triphosphatase. *J. Biol. Chem.* 262:16338–16342.

Inesi, G., L. Chen, C. Sumbilla, D. Lewis, and M. E. Kirtley. 1995. Ca^{2+} binding and translocation by the sarcoplasmic reticulum ATPase: functional and structural considerations. *Biosci. Rep.* 15:327–339.

Inesi, G., and L. de Meis. 1989. Regulation of steady state filling in sarcoplasmic reticulum. *J. Biol. Chem.* 264:5929–5936.

Inesi, G., C. Sumbilla, and M. E. Kirtley. 1990. Relationships of molecular structure and function in Ca^{2+}-transport ATPase. *Physiol. Rev.* 70: 749–760.

Klodos, I., and B. Forbush, III. 1988. Rapid conformational changes of the Na/K pump revealed by a fluorescent dye RH-160. *J. Gen. Physiol.* 92:46a.

Läuger, P. 1991. Electrogenic Ion Pumps. Sinauer Assoc., Sunderland, MA. 1–313.

MacLennan, D. H., W. J. Rice, and N. M. Green. 1997. The mechanism of Ca^{2+} transport by sarco(endo)plasmic reticulum Ca^{2+}-ATPases. *J. Biol. Chem.* 272:28815–28818.

Markwell, M. A., S. M. Haas, L. L. Bieber, and N. E. Tolbert. 1978. A modification of the Lowry procedure to simplify protein determination in membrane and lipoprotein samples. *Anal. Biochem.* 87:206–210.

Martonosi, A. 1995. The structure and interactions of Ca^{2+}-ATPase. *Biosci. Rep.* 15:263–281.

Menguy, T., F. Corre, L. Bouneau, S. Deschamps, J. V. Møller, P. Champeil, M. le Maire, and P. Falson. 1998. The cytoplasmic loop located between transmembrane segments 6 and 7 controls activation by Ca^{2+} of sarcoplasmic reticulum Ca^{2+}-ATPase. *J. Biol. Chem.* 273: 20134–20143.

Møller, J. V., B. Juul, and M. le Maire. 1996. Structural organization, ion transport, and energy transduction of P-type ATPases. *Biochim. Biophys. Acta.* 1286:1–51.

Schneeberger, A., and H.-J. Apell. 1999. Ion selectivity of the cytoplasmic binding sites of the Na,K-ATPase: I. Sodium binding is associated with a conformational rearrangement. *J. Membr. Biol.* 168:221–228.

Schneeberger, A., and H.-J. Apell. 2001. Ion selectivity of the cytoplasmic binding sites of the Na,K-ATPase: II. Competition of various cations. *J. Membr. Biol.* 179:263–273.

Schwartz, A. K., M. Nagano, M. Nakao, G. E. Lindenmayer, and J. C. Allen. 1971. The sodium- and potassium-activated adenosinetriphosphatase system. *Meth. Pharmacol.* 1:361–388.

Stürmer, W., R. Bühler, H.-J. Apell, and P. Läuger. 1991. Charge translocation by the Na,K-pump: II. Ion binding and release at the extracellular face. *J. Membr. Biol.* 121:163–176.

Toyoshima, C., M. Nakasako, H. Nomura, and H. Ogawa. 2000. Crystal structure of the calcium pump of sarcoplasmatic reticulum at 2.6 Å resolution. *Nature.* 405:647–655.

Vilsen, B. 1995. Structure–function relationships in the Ca^{2+}-ATPase of sarcoplasmic reticulum studied by use of the substrate analogue CrATP and site-directed mutagenesis. Comparison with the Na^+,K^+-ATPase. *Acta Physiol. Scand. Suppl.* 624:1–146.

Yu, X., S. Carroll, J.-L. Rigaud, and G. Inesi. 1993. H^+ countertransport and electrogenicity of the sarcoplasmic reticulum Ca^{2+} pump in reconstituted proteoliposomes. *Biophys. J.* 64:1232–1342.

Yu, X., L. Hao, and G. Inesi. 1994. A pK change of Acidic residues contributes to cation countertransport in the Ca-ATPase of Sarcoplasmic Reticulum. *J. Biol. Chem.* 269:16656–16661.

Yu, X., and G. Inesi. 1995. Variable stoichiometric efficiency of Ca^{2+} and Sr^{2+} transport by the sarcoplasmic reticulum ATPase. *J. Biol. Chem.* 270:4361–4367.

Zhang, P., C. Toyoshima, K. Yonekura, N. M. Green, and D. L. Stokes. 1998. Structure of the calcium pump from sarcoplasmic reticulum at 8-Å resolution. *Nature.* 392:835–839.